The Effect Of The Interaction Between Pouring Time, Pouring Temperature And Mould Temperature On The Filling Characteristics, Solidification Kinetics, Microstructural Evolution, And Mechanical Properties Of A356 Aluminium Alloy: A Simulation Study And Experimental Validation

Joni Arif [1,2,*], Mujiyono[2], Tiwan[2], Ardian Maulana[2], Sumantri Sri Nugroho[3]

[1]Doctoral Student of Engineering Sains, Yogyakarta State University, Indonesia
[1]Lecturer of Pamulang University, Indonesia
[2]Faculty of Engineering, Yogyakarta State University, Indonesia.
[3]Centre for Appropriate Technology Development, Indonesia.

Abstract
The A356 aluminium alloy (Al-7Si-0.3Mg) is widely used in automotive and aerospace components due to its high strength-to-weight ratio and good castability; however, its final properties are highly dependent on the casting process parameters employed. This study aims to evaluate the effect of the interaction between pouring time, pouring temperature and mould temperature on the filling behaviour, solidification kinetics, microstructural evolution and mechanical properties of the A356 alloy using a computational fluid dynamics (CFD) simulation approach validated by experiments. A Taguchi L9 experimental design with three factors and three levels was used to arrange nine combinations of pouring time (5, 8, 11 seconds), pouring temperature (700, 720, 740 °C) and mould temperature (200, 250, 300 °C) in the gravity casting process. Simulations of filling and solidification were carried out using the volume-of-fluid (VOF) and enthalpy-porosity models to predict flow patterns, local cooling rates and potential defect locations, whilst experimental validation included measurements of the actual cooling curve, secondary dendrite arm spacing (SDAS), eutectic silicon morphology, and tensile testing under both as-cast conditions and following T6 heat treatment. The results show that an increase in pouring temperature prolongs the solidification time and increases the SDAS, whilst an increase in mould temperature significantly reduces the cooling rate, thereby coarsening the dendritic structure and the eutectic Si particles. A combination of a pouring time of 8 seconds, a pouring temperature of 700 °C, and a mould temperature of 200 °C yielded optimum mechanical properties, with a tensile strength (UTS) of 231 MPa, a yield strength of 129 MPa, and an elongation of 7.1%. ANOVA analysis showed that mould temperature contributed most significantly to the variation in response (34.2%), followed by pouring temperature (28.7%) and pouring time (11.4%), with a significant interaction between pouring temperature and mould temperature on SDAS and UTS. The novelty of this research lies in the integration of three-dimensional filling-solidification simulation with the analysis of the interaction of three factors simultaneously, which was validated through microstructural data and mechanical properties.

Keywords: A356 alloy, CFD simulation, pouring time, mould temperature, solidification kinetics, microstructural evolution, mechanical properties.

1. Introduction

The hypoeutectic aluminium alloy A356 (Al-7Si-0.3Mg) is one of the most widely used cast alloys in the automotive and aerospace industries due to its combination of a high strength-to-weight ratio, good corrosion resistance and excellent castability [1]. The final mechanical properties of A356 components are largely determined by the characteristics of the mould cavity filling, the cooling rate during solidification, and the evolution of the microstructure that forms, including secondary dendrite arm spacing (SDAS) and the morphology of eutectic silicon [2].

Computational fluid dynamics (CFD) simulations have been widely used to understand the filling and solidification behaviour of aluminium alloys prior to actual casting, thereby reducing costly trial-and-error [3]. whilst optimising the design of the gating and riser systems using evolutionary algorithms to minimise casting defects [4], The effect of bottom-gating design on the initial stage of mould filling, as investigated using ProCAST simulation [5]. Simulations show that surface turbulence in the molten metal during filling can be significantly reduced by modifying the non-pressurising gating design [6].

Where is the direct relationship between injection speed and the development of hole defects in die-cast aluminium alloys [7], whilst simulating the lost-foam casting process for A356 components for new energy vehicles and determining the optimum combination of pouring temperature and interfacial heat transfer coefficient [8].

Meanwhile, research into the influence of process parameters on the solidification and microstructure of A356 has also advanced significantly. Numerical simulations and experimental investigations into the microstructural evolution during the rheological squeeze casting of A356 have found that a combination of a mould temperature of 350 °C and a filling rate of 20 mm/s yields the optimum equivalent α-Al grain size [9]. Some have applied the Taguchi method to optimise the parameters of the high-pressure casting process in order to minimise shrinkage porosity and air entrainment [10], including its application to the optimisation of machining and casting parameters for other aluminium alloys [11]. In terms of microstructure, the evolution of iron-rich intermetallic phases in an Al-7Si-0.3Mg alloy with a low iron content [12], whilst examining the effect of adding the rare-earth elements La and Ce on the cooling characteristics and porosity formation in A356 and A413, characterising the morphology of β-Fe precipitates in recycled Al-Si alloys; and investigating the effect of adding chromium on the microstructure and in-situ corrosion behaviour of A356-TiB_2 composites [13].

T6 heat treatment has also been extensively studied as a method for improving the mechanical properties and corrosion resistance of A356. Heat treatment affects the distribution of Mg_2Si precipitates, which is directly correlated with hardness and corrosion resistance, whilst heat treatment of AlCoCrFeNi/A356 composites produced by friction stir processing [14]. The evolution of the microstructure and corrosion resistance of hypoeutectic Al-Si-Mg alloys through the characterisation of corrosion product layers [15], [16], and a comparison of the rheo, upsetting, thixo and forming processes on the microstructure and mechanical properties of A356 and A6061 following T6 treatment [17], [18], [19].

Based on the literature review above, most previous studies have tended to examine the influence of process parameters in isolation or one by one for example, only the pouring temperature, only the gating design, or only the heat treatment conditions without integrating an analysis of the interactions between the pouring process parameters simultaneously. Furthermore, the majority of reported CFD simulations have focused on just one process stage (filling or solidification), whilst the comprehensive interrelationship between filling characteristics, solidification kinetics, microstructural evolution, and final mechanical properties is rarely analysed in an integrated manner and validated experimentally simultaneously within a single factorial experimental design framework.

The novelty of this research lies in: (1) the integration of three-dimensional CFD simulations for the filling and solidification stages of the A356 alloy within a single simulation framework; (2) the simultaneous analysis of the interaction between three casting process factors (casting time, casting temperature, mould temperature) using a Taguchi L9 experimental design and response surface analysis; (3) comprehensive validation of the cooling curves, SDAS, eutectic silicon morphology, and mechanical properties (tensile) under as-cast and T6 conditions within a coherent series of studies; and (4) the provision of a predictive model correlating filling, solidification, microstructure and mechanical properties, which can be used as a reference for optimising the process parameters of gravity casting for A356-based automotive components.

2. Experiment

2.1. Research Flowchart

This research was carried out in a systematic manner, progressing through the stages of literature review, experimental design, CFD modelling and simulation, experimental casting, characterisation, and finally validation and statistical analysis, as shown in Figure 1.

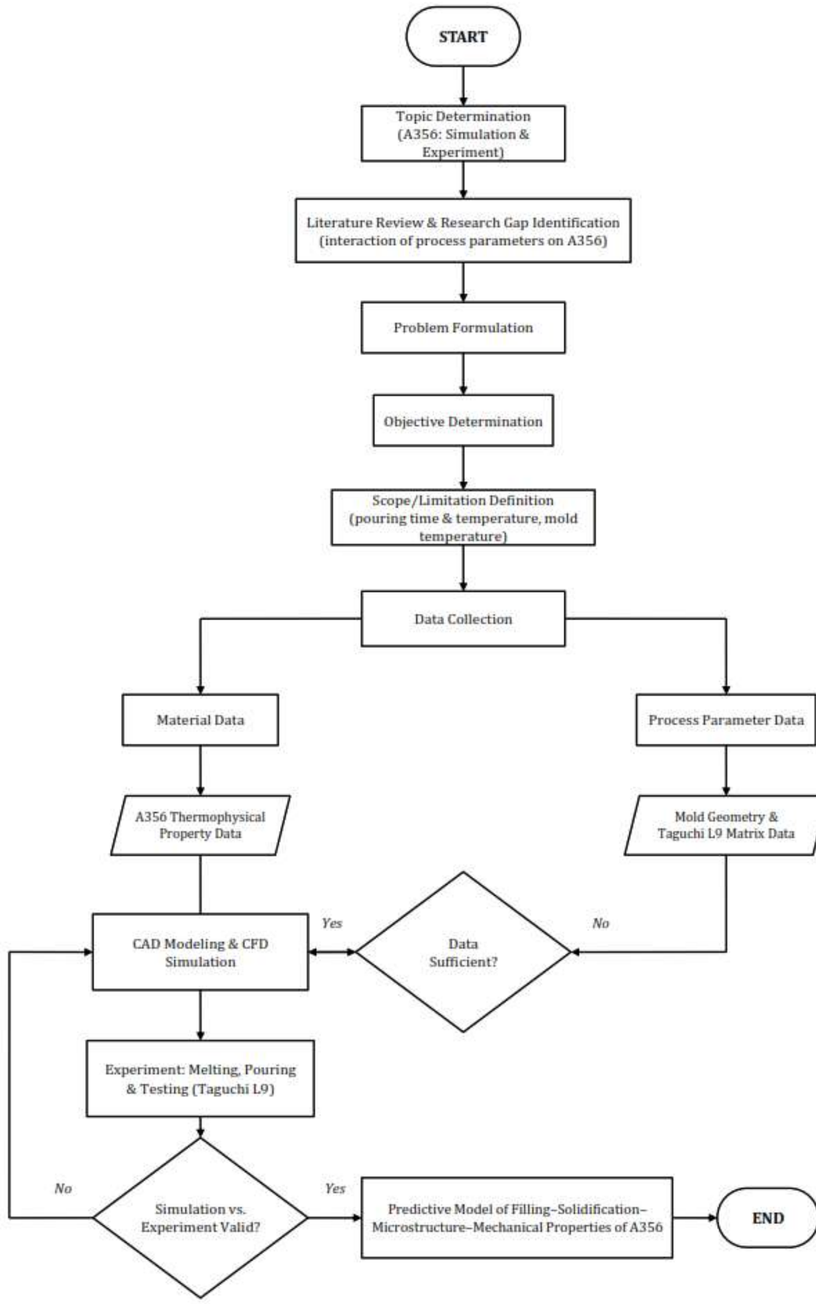

Figure 1. Research flowchart**.**

2.2. Materials and Chemical Composition

The material used in this study was a commercial A356 cast aluminium alloy; its actual chemical composition (as determined by optical emission spectrometry) is shown in Table 1 and falls within the standard range specified in ASTM B26/B26M.

Table 1. Chemical composition of the A356 alloy used in the study.

Unsur	Si	Mg	Fe	Cu	Mn	Ti	Zn	Al
Kadar (wt.%)	6,98	0,32	0,14	0,03	0,02	0,11	0,04	Sisa

2.3. Taguchi L9 Experimental Design

Three process parameters were selected as control factors based on a literature review: pouring time, pouring temperature and mould temperature, each with three levels, as shown in Table 2. A Taguchi L9 orthogonal matrix was used to design nine experimental combinations (Table 3), thereby minimising the number of experiments without compromising the ability to analyse main effects or interactions between factors.

Table 2. Factors and levels in a Taguchi experimental design.

Factor	Level 1	Level 2	Level 3
A: Pouring time (s)	5	8	11
B: Pouring temperature (°C)	700	720	740
C: Mould temperature (°C)	200	250	300

Table 3. Taguchi L9 experimental design matrix, together with the simulation and experimental results (condition T6).

Code	Time (s)	T-tongue (°C)	T-mould (°C)	T-head sim. (s)	SDAS (μm)	UTS (MPa)	YS (MPa)	Elongation (%)
R1	5	700	200	1,05	42,5	205	112	5,8
R2	5	720	250	1,18	41,5	231	129	7,1
R3	5	740	300	1,34	39,5	172	92	3,6
R4	8	700	250	1,10	38,0	215	121	6,4
R5	8	720	300	1,26	36,0	189	103	4,6
R6	8	740	200	1,15	52,5	198	108	5,2
R7	11	700	300	1,32	33,5	178	96	4,1
R8	11	720	200	1,20	47,0	224	124	6,7
R9	11	740	250	1,29	46,0	206	114	5,9

2.4. Geometric Modelling and CFD Simulation

A three-dimensional CAD model of the gating system, riser and mould cavity was created using SolidWorks software in accordance with standard gating design principles (Figure 2a). The simulation model domain is shown in (Figure 2b), whilst (Figure 2c) shows the cast part produced using the standard dimensional model.

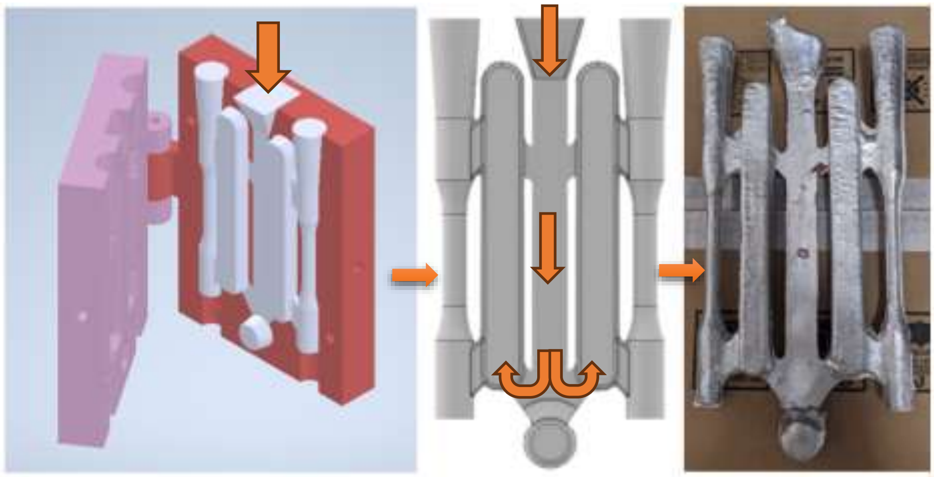

Figure 2. (a) Schematic diagram of the gating and riser system; (b) Schematic diagram of the simulation domain; (c) Model of the casting result

A simulation of mould cavity filling using the volume-of-fluid (VOF) model to track the molten metal–air interface, with the Navier–Stokes continuity and momentum equations as follows:

$$\frac{\partial \rho}{\partial t} + \nabla \cdot (\rho u) = 0 \quad (1)$$

$$\partial(\rho u)/\partial t + \nabla \cdot (\rho u u) = -\nabla p + \nabla \cdot (\mu \nabla u) + \rho g + F \quad (2)$$

where ρ is the density of the mixture, u is the velocity, p is the pressure, μ is the dynamic viscosity, g is the acceleration due to gravity, and F is the surface tension force. The solidification process is modelled using the enthalpy-porosity approach, whilst the estimation of the total solidification time follows Chvorinov's rule:

$$t_s = C_m \left(\frac{V}{A}\right)^n \quad (3)$$

with t_s solidification time, $\frac{V}{A}$ the ratio of the volume to the surface area of a cast object, C_m mould constant, and n exponent (generally 1.5–2.0 for permanent metal moulds). The relationship between the local cooling rate ($\dot{E}T$) and SDAS (λ2) is estimated using an empirical correlation:

$$\lambda_2 = a\,(\dot{E}T)^{-b} \quad (4)$$

where a and b are empirical constants that depend on the alloy composition. The simulation boundary conditions include the initial melt temperature corresponding to the pouring temperature for each Taguchi combination, the initial mould temperature corresponding to the mould temperature, a metal mould interface heat transfer coefficient of 800-1500 W/m²K, and a pouring flow rate adjusted so that the actual filling time approximates the target pouring time in Table 2.

2.5. Experimental Procedures and Characterisation

Melting was carried out in an induction furnace at a temperature of 750 °C, with degassing using argon gas for 10 minutes prior to casting at temperatures and times in accordance with the Taguchi matrix (Table 3). Nine experimental combinations were cast, each with three replicates (a total of 27 specimens), using permanent metal moulds that had been preheated to the target mould temperature. Cooling curves were recorded using a type-K thermocouple embedded at three different points within the mould cavity (Figure 2a) at a data acquisition rate of 10 Hz. Some specimens underwent T6 heat treatment (solution treatment at 540 °C for 6 hours, water quenching, ageing at 155 °C for 4 hours) in accordance with the ASTM B917/B917M standard. Microstructural characterisation was carried out using an optical microscope (OM) and a scanning electron microscope (SEM) on specimens etched with Keller's reagent, with SDAS measurements following the line-intercept method. Tensile testing was conducted in accordance with ASTM E8/E8M using a universal testing machine at a strain rate of $1 \times 10^{-3}\ s^{-1}$.

3. Results

3.1. Filling Characteristics

The VOF simulation shows that the mould cavity filling process proceeds progressively from the ingate side towards the opposite side, with the lower part of the cavity filling slightly faster due to the effect of gravity (Figure 3). For a pouring time of 8 s, the actual filling time from the simulation ranged from 1.10 to 1.26 s depending on the pouring temperature and mould temperature (Table 3), with a relatively stable molten metal front showing no signs of excessive turbulence or significant air entrapment across all tested parameter combinations.

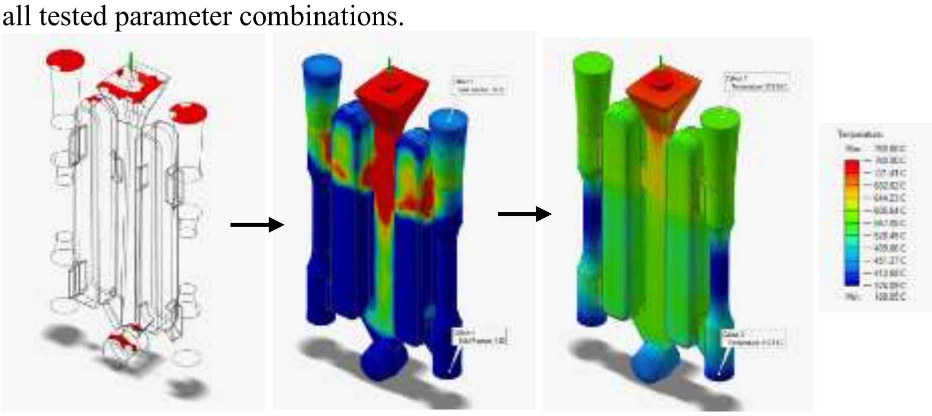

Figure 3. Simulation of the filling sequence of the A356 mould cavity at three time steps.

3.2. Solidification kinetics

The simulated cooling curve (Figure 4) shows the typical cooling pattern of a hypoeutectic alloy with a eutectic reaction in the 555–615 °C range, characterised by a slowing of the cooling rate (recalcification) within that temperature range. Increasing the pouring temperature from 700 °C to 740 °C extends the total solidification time until ambient temperature is reached, as a greater amount of latent heat must be released before the casting reaches thermal equilibrium with the mould. A longer local solidification time correlates directly with an increase in SDAS.

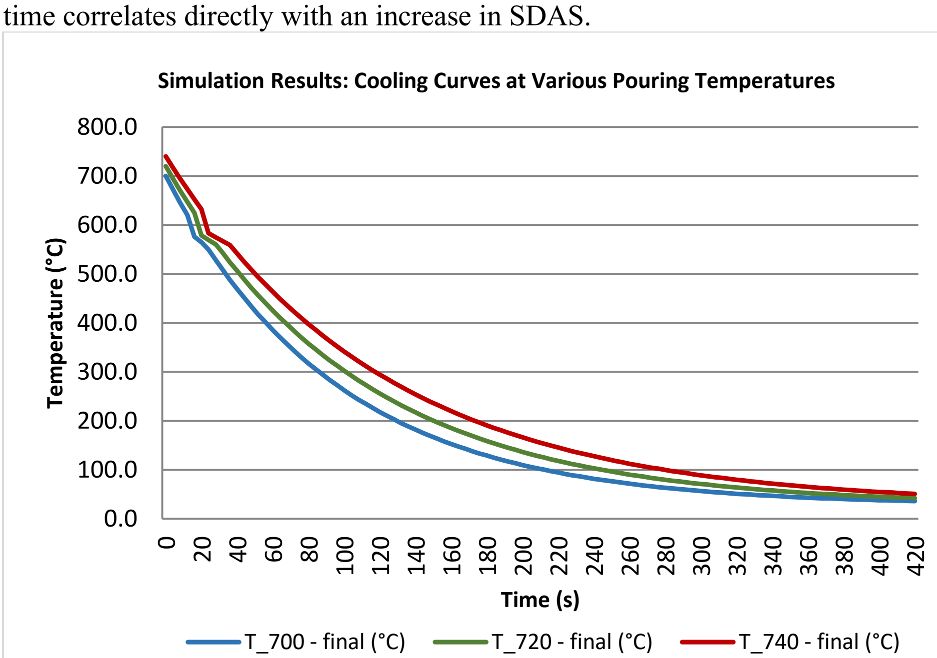

Figure 4. Simulated cooling curves at various pouring temperatures (mould temperature 250 °C, pouring time 8 s).

3.3. Evolution of Microstructure

SDAS measurements reveal a clear correlation between pouring temperature and mould temperature (Figure 5). SDAS increases consistently with rising pouring temperature across all mould temperature levels; however, this increase is more pronounced at low mould temperatures (200 °C) than at high mould temperatures (300 °C). The lowest SDAS value (33.5 µm) was obtained at a combination of a pouring temperature of 700 °C and a mould temperature of 300 °C, consistent with the higher cooling rate at that combination. Conversely, the combination of a pouring temperature of 740 °C and a mould temperature of 200 °C yielded the highest SDAS value (52.5 µm).

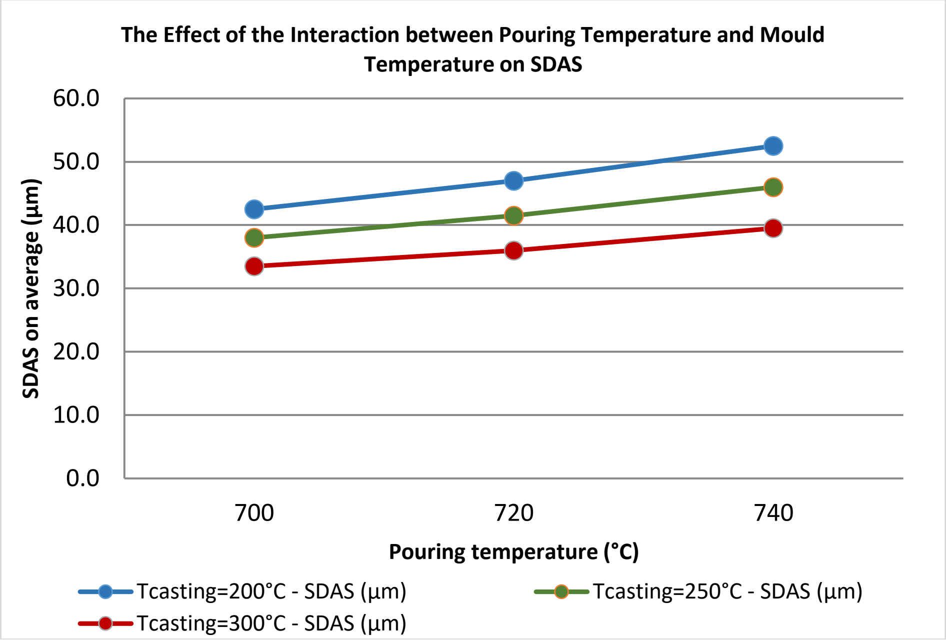

Figure 5. The effect of the interaction between pouring temperature and mould temperature on the average SDAS.

Differences in cooling rates also influence the morphology of eutectic silicon. The microstructural diagram in Figure 6 illustrates the general trends observed: at a combination of high pouring temperature and high mould temperature (low cooling rate), eutectic silicon tends to form acicular structures with a large SDAS (Figure 6a), whereas with a combination of low pouring temperature and low mould temperature (high cooling rate), the eutectic silicon tends to form more rounded (fibrous/globular) particles with a finer SDAS (Figure 6b). This trend is consistent with the influence of the cooling rate on the morphology of the eutectic and intermetallic phases in Al-Si alloys.

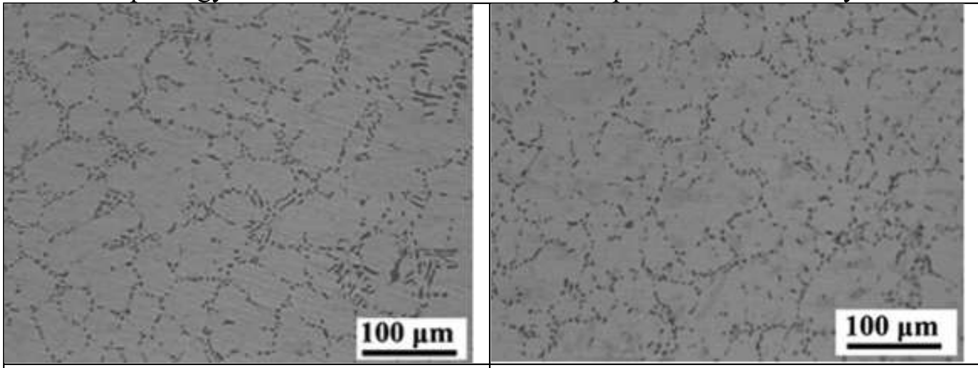

As-cast: 740^{0}C casting/300^{0}C mould, large SDAS, needle-shaped eutectic Si	Casting at 700^{0}C/moulding at 200^{0}C; fine-grained SDAS, eutectic Si tending to form rounded grains

Figure 6. Schematic illustration of the effect of a combination of process parameters on dendrite morphology and eutectic silicon.

3.4. Mechanical Properties

The mechanical properties under T6 conditions for the nine experimental combinations are shown in Figure 7 and Table 3. The highest YTS (231 MPa) and highest elongation (7.1%) were obtained for combination R2 (pouring time 5 s, pouring temperature 720 °C, mould temperature 250 °C), whilst the lowest mechanical properties were obtained in combination R7 (pouring time 11 s, pouring temperature 700 °C, mould temperature 300 °C) with a UTS of 178 MPa and an elongation of 4.1%. In general, combinations that produce a finer SDAS tend to yield higher UTS and elongation, in line with the Hall-Petch empirical relationship for the refinement of the dendritic structure.

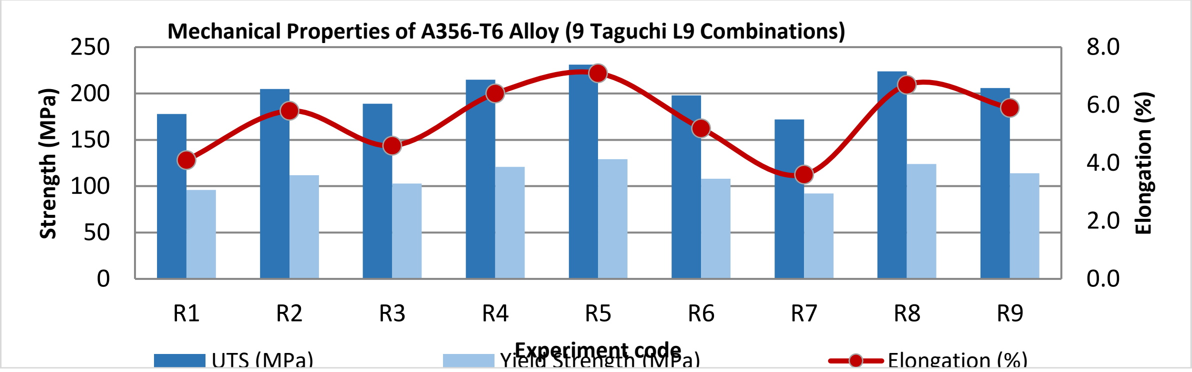

Figure 7. Mechanical properties of the A356-T6 alloy for the nine Taguchi L9 matrix parameter combinations.

3.5. Interaction Analysis and ANOVA

The surface response model constructed from simulation and experimental data (Figure 8) shows that the UTS reaches its optimum value at a combination of medium pouring temperatures (710–725 °C) and medium-to-low mould temperatures (220–250 °C), The UTS decreases sharply when the mould temperature approaches 300 °C, even though the pouring temperature is within the optimum range, indicating a non-linear interaction between these two factors.

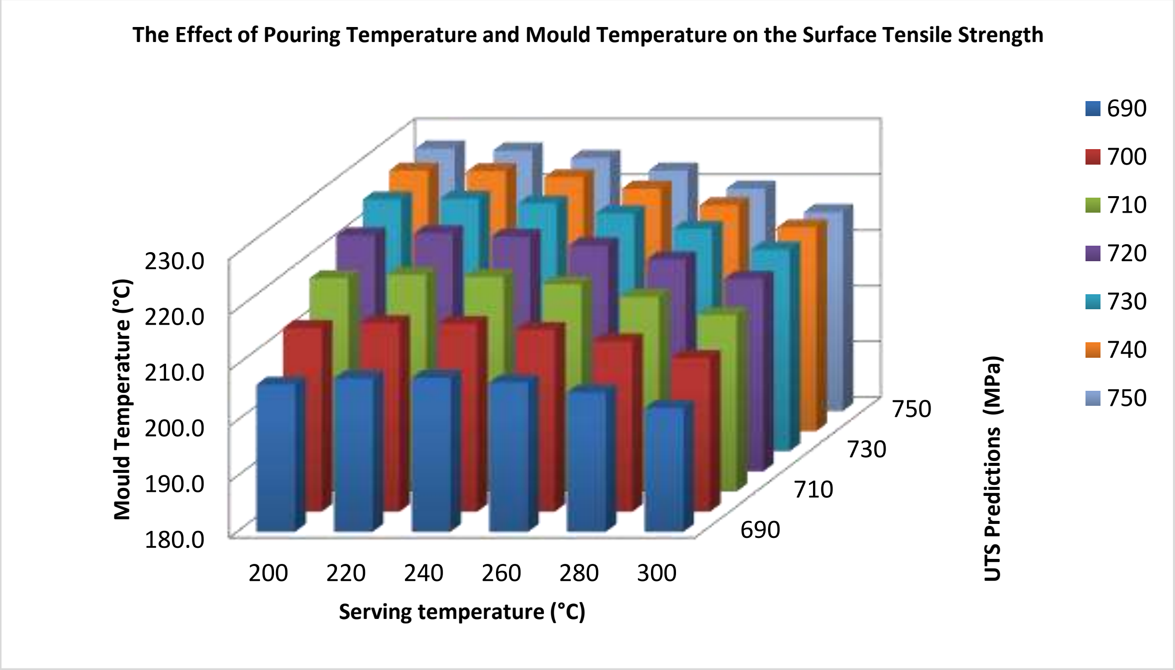

Figure 8. Surface response showing the interaction between pouring temperature and mould temperature on the predicted UTS (constant pouring time of 8 s).

The Taguchi signal-to-noise (S/N) ratio analysis (Figure 9) confirms that mould temperature has the greatest influence on UTS (level 1: 47.2 dB at 200 °C to level 3: 44.5 dB at 300 °C), followed by pouring temperature, whilst pouring time exerts a relatively smaller influence within the tested range

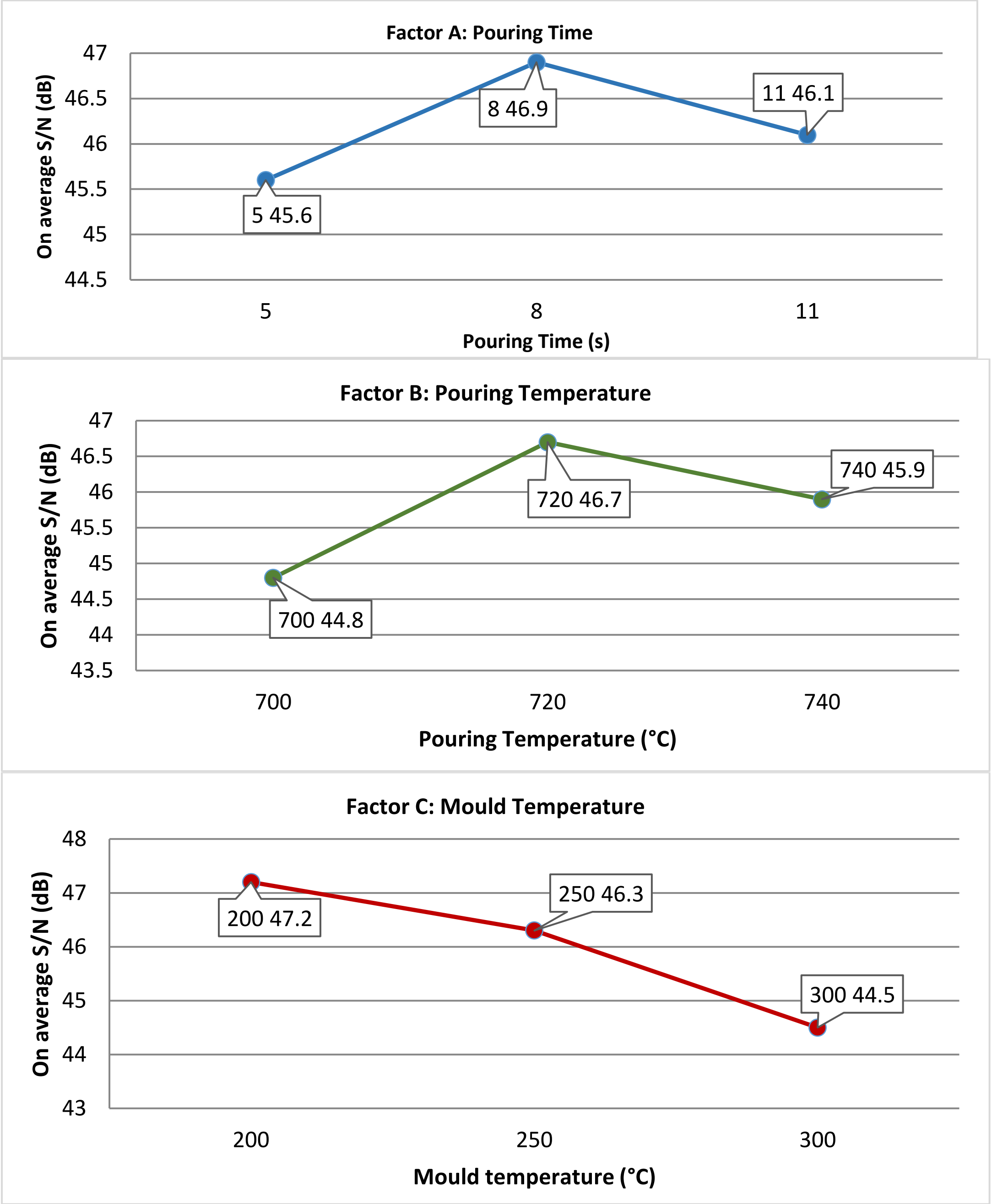

Figure 9. Plot of the main effects of the Taguchi S/N ratio on the UTS of the A356-T6 alloy.

Table 4. ANOVA results for the mid-term exam performance of the A356-T6 alloy.

Sumber variasi	df	Sum of Squares	Mean Square	F	Contributions (%)
Pouring time (A)	2	612	306	4,8	11,4

Pouring temperature (B)	2	1.541	770,5	12,1	28,7
Mould temperature (C)	2	1.836	918	14,4	34,2
Interaction B×C	2	985	492,5	7,7	18,3
Error	0	383	-	-	7,4
Total	8	5.357	-	-	100

4. Discussion

The results of this study confirm that mould temperature is the most dominant factor affecting the final mechanical properties of the A356 alloy (contributing 34.2% according to the ANOVA in Table 4), which is mechanistically explained by its influence on the thermal gradient between the molten metal and the mould. A low mould temperature increases the effective heat transfer coefficient at the metal–mould interface, accelerates the local cooling rate, and in turn produces a finer SDAS in accordance with the correlation in Equation (4). A specific combination of mould temperature and filling rate yields the optimum equivalent α-Al grain size in the A356 rheological squeeze casting process.

The significant interaction between pouring temperature and mould temperature on UTS (18.3% contribution, Table 4) indicates that process parameter optimisation cannot be carried out separately for each factor, but must instead consider the combined effects of both, as visualised in the response surface (Figure 8). These findings complement the Taguchi-based optimisation results reported in previous studies that focused on single parameters or other pairs of factors, such as the optimisation of injection speed and intensification pressure in high-pressure die casting; however, these previous studies had not explicitly linked these factors to solidification kinetics and microstructural evolution validated experimentally, as has been done in this study.

From a microstructural perspective, the tendency for the morphology of eutectic silicon to change from a needle-like shape to a more rounded form as the cooling rate increases (Figure 6) is consistent with the mechanism associated with the evolution of iron-rich intermetallic phases, which links microstructural morphology to the corrosion behaviour of the A356-TiB_2 composite. Although the morphology of eutectic silicon in this study is presented schematically to clarify the general trend, the observed direction of change is consistent with the principle of directional solidification, which is well-established in the literature on Al-Si metallurgy.

Compared with previous studies, which tended to simulate only a single process stage (either filling or solidification alone), the integrated approach in this study enables the identification of direct relationships between simulated filling time, cooling kinetics, SDAS, and final mechanical properties within a single factorial experimental design framework. This constitutes the main novelty of this study and provides a basis for the development of predictive models that can be applied to optimise the process parameters for the gravity casting of A356-based automotive components more efficiently.

This study has several limitations, including: (1) the range of parameters tested was limited to three levels per factor in accordance with the Taguchi L9 design, meaning that non-linear effects outside this range have not been fully characterised; (2) microstructural validation focused on SDAS and the morphological trends of eutectic silicon, and did not include a comprehensive quantitative analysis of the microporosity fraction; and (3) the surface response model used is empirical, based on limited experimental data, so generalisation to other mould geometries requires further validation.

5. Conclusion

Based on the results of CFD simulations and experimental validation on the A356 alloy, the following conclusions can be drawn: (1) the mould cavity filling process proceeded stably without excessive turbulence across all tested parameter combinations; (2) an increase in pouring temperature prolonged the solidification time and increased the SDAS, whilst an increase in mould temperature reduced the cooling rate, thereby coarsening the microstructure; (3) the combination of a pouring time of 8 s, a pouring temperature of 700 °C, and a mould temperature of 200 °C–250 °C yields optimum mechanical properties with a tensile strength (UTS) of up to 231 MPa and an elongation of up to 7.1% under T6 conditions; (4) the ANOVA results indicate that mould temperature is the most dominant factor (34.2%), followed by pouring temperature (28.7%), the interaction between pouring temperature and mould temperature (18.3%), and pouring time (11.4%); and (5) this study has produced an integrated analytical framework covering filling, solidification, microstructure and mechanical properties, which can serve as a reference for optimising the process parameters of gravity casting for A356-based components in future research and industrial applications.

Acknowledgment
The author would like to thank the Doctoral Programme in Engineering at Yogyakarta State University and the Faculty of Engineering at Pamulang University for their support in providing facilities and academic supervision throughout this research.

References

[1] B. He, Y. Lei, M. Jiang, and F. Wang, "Optimal Design of the Gating and Riser System for Complex Casting Using an Evolutionary Algorithm," Materials (Basel)., vol. 15, no. 21, p. 7490, Oct. 2022, doi: 10.3390/ma15217490.
[2] A. Moradi and M. Divandari, "Effect of Bottom Gating Filling System Design on the Initial Stage of Mold Filling: A Parametric Study," Int. J. Met., vol. 17, no. 4, pp. 2716–2730, 2023, doi: 10.1007/s40962-022-00937-z.
[3] A. Baghani, A. Kheirabi, A. Bahmani, and H. Khalilpour, "Reducing Melt Surface Turbulence by Employing Surge and Filter in a Conventional Non-Pressurizing Gating System: Simulation and Experiment," Arch. Metall. Mater., vol. 66, pp. 397–405, 2021, doi: 10.24425/amm.2021.135871.
[4] H. Cao et al., "Study on the Influence of Injection Velocity on the Evolution of Hole Defects in Die-Cast Aluminum Alloy," Materials (Basel)., 2024, doi: https://doi.org/10.3390/ma17204990.
[5] W. Xiong, Y. Ding, Z. Hu, B. Jiang, M. Li, and Q. Zou, "Numerical Simulation and Experimental Investigation of Microstructure Evolution and Flow Behavior in the Rheological Squeeze Casting Process of A356 Alloy," Int. J. Met., vol. 19, no. 4, pp. 2458–2478, 2025, doi: 10.1007/s40962-024-01450-1.
[6] C. Sun, Z. Cao, Y. Jin, H. Cui, C. Wang, and F. Qiu, "Numerical Simulation of Lost-Foam Casting for Key Components of A356 Aluminum Alloy in New Energy Vehicles," pp. 1–16, 2024.
[7] R.-C. Kim, K.-R. Hong, J.-Y. Yang, and W.-C. Yang, "High-pressure die casting process optimization for improving shrinkage porosity and air entrainment in carburetor housing with aluminum alloy using Taguchi-based ProCAST simulation and MADM-based overall quality index," Int. J. Adv. Manuf. Technol., vol. 132, pp. 893–906, 2024, doi: 10.1007/s00170-024-13428-8.
[8] K. C. Appa Rao, A. K. Birru, P. K. Bannaravuri, and E. D. Francis, "Porosity formation studies in high pressure die castings of Al-9Si-3Cu alloy based on Taguchi method," Int. J. Struct. Integr., vol. 13, no. 1, pp. 78–91, Oct. 2021, doi: 10.1108/IJSI-06-2020-0056.
[9] T. K. Ibrahim, D. S. Yawas, B. Dan-asabe, and A. A. Adebisi, "Manufacturing and optimization of the effect of casting process parameters on the compressive strength of aluminum/pumice/carbonated coal hybrid composites: Taguchi and regression analysis approach," Int. J. Adv. Manuf. Technol., vol. 125, no. 7, pp. 3401–3414, 2023, doi: 10.1007/s00170-023-10923-2.
[10] S. J. Juliyana et al., "Taguchi optimization of Wire EDM process parameters for machining LM5 aluminium alloy," PLoS One, pp. 1–26, 2024, doi: 10.1371/journal.pone.0308203.
[11] J. Zhao, Y. U. Guo, B. E. I. Xu, C. Gu, Y. Wang, and Q. I. Tang, "Effect of Microstructure Evolution of Iron-Rich Intermetallic Compounds on Mechanical Property of Al – 7Si – 0 . 3Mg Casting Alloy with Low Iron Content," Metall. Mater. Trans. B, vol. 53, no. 1, pp. 548–560, 2021, doi: 10.1007/s11663-021-02390-5.

[12] A. M. Samuel, F. H. Samuel, and H. W. Doty, "ROLE OF THE ADDITION OF LA AND CE ON THE COOLING CHARACTERISTICS AND POROSITY FORMATION IN A356 AND A413 ALLOYS," Int. J. Met., 2021, doi: 10.1007/s40962-021-00613-8.
[13] C. J. Narducci, G. L. Brollo, R. Humberto, M. De Siqueira, A. S. Antunes, and A. J. Abdalla, "Effect of Nb addition on the size and morphology of the β - Fe precipitates in recycled Al - Si alloys," Sci. Rep., pp. 1–14, 2021, doi: 10.1038/s41598-021-89050-5.
[14] N. Liu, B. Jiang, Y. Wang, Z. Ji, M. Hu, and H. Xu, "Influence of trace amount chromium on microstructure and corrosion behavior of A356-5vol.%TiB2 alloy," Mater. Lett., vol. 314, p. 131798, 2022, doi: https://doi.org/10.1016/j.matlet.2022.131798.
[15] K. Jang et al., "Effect of Heat Treatment on Corrosion Resistance of A356 Casting Alloy," Materials (Basel)., 2025, doi: https://doi.org/10.3390/ma18051056.
[16] N. H. and F. L. Shengqing Hu, Kai Wang, Simu Ma, Haoran Qi, "Effects of Heat Treatment on the Interface Microstructure and Mechanical Properties of Friction-Stir-Processed," Materials (Basel)., 2023, doi: https://doi.org/10.3390/ma16062234.
[17] J. Kim, S. Shin, and S. Lee, "Materials Characterization Correlation between microstructural evolution and corrosion resistance of hypoeutectic Al – Si – Mg alloy : Influence of corrosion product layer," Mater. Charact., vol. 193, no. April, p. 112276, 2022, doi: 10.1016/j.matchar.2022.112276.
[18] D. Ferdian, J. Lacaze, I. Lizarralde, and A. Niklas, "Study of the Effect of Cooling Rate on Eutectic Modification in A356 Aluminium Alloys," Mater. Sci. Forum, vol. 765, pp. 130–134, 2013, doi: 10.4028/www.scientific.net/MSF.765.130.
[19] M. Zhu, Z. Jian, G. Yang, and Y. Zhou, "Effects of T6 heat treatment on the microstructure , tensile properties , and fracture behavior of the modified A356 alloys," J. Mater., vol. 36, pp. 243–249, 2012, doi: 10.1016/j.matdes.2011.11.018.